

# Design and Implementation of Improved Fractal Loop Antennas for Passive UHF RFID Tags Based on Expanding the Enclosed Area

Qusai H. Sultan and Ahmed M. A. Sabaawi\*

**Abstract**—In this paper, new fractal curves are designed, simulated, and implemented for passive UHF RFID application. 5-, 6-, 7-, and 8-sides polygon fractal loops are proposed and implemented in this work based on the 2nd iteration. It is shown that increasing the number of sides can improve the performance and minimize the size of the fractal antenna. The designed fractal loop antennas have been compared with other fractal loop antennas published previously, and the recent antennas show a better performance. The designed antennas are fabricated using PCB technology, and the antenna parameters are measured experimentally and compared to CST simulations. There is an acceptable agreement between the simulated and measured results. The effect of different materials on antenna performance is also studied.

## 1. INTRODUCTION

Automatic identification (Auto-ID) techniques have received significant interest from researchers in the last few decades due to the popularity of many services and industries such as: sales logistic, supply chain, and manufacturing industry. Auto-ID systems help in gathering information about products and goods in transit as well as tracking people and animals. Although omnipresent barcode labels were considered as a revolutionary identification technology for many years because they are simple and cheap, barcode labels have been found inadequate in an increasing number of cases [1]. Barcodes are not programmable and have low storage, which make them a step behind the current fast developing demand on rapid and efficient identification systems. A typical solution would be storing the data in a small and inexpensive electronic chip through a wireless transfer of data between the tag and the reader. Ideally, the power required to operate the electronics in the tag will be provided and transmitted by the reader. The contactless identification systems are so called backscattered Radio Frequency Identification systems (RFID) [2].

The focus in this paper is on passive UHF RFID tags where the reader and the passive tag communicate with each other through backscattered EM waves. Passive tags have an electronic chip integrated with a UHF antenna packaged together. The tag packaging determines the reliability and tolerance, where the antenna type and design determine the wireless communication capability when the tag is attached to the object to be identified. Several antenna designs have been proposed and developed over decades; however, there are still many challenges nowadays such as tagging different objects made of metal or another conductive material while keeping the performance consistent. Conductive materials such as metals have a strong impact on the antenna performance by degrading the radiation efficiency. Objects made of metals, such as aluminum cans, are commonly utilized in many industries that employ passive RFID systems. Thus, tag antennas should fulfill the minimum operating conditions and be designed to perform well when being placed on different objects made of different materials without performance degradation. Generally, omnidirectional antennas are preferred in this application to ensure

---

*Received 22 January 2021, Accepted 22 March 2021, Scheduled 27 March 2021*

\* Corresponding author: Ahmed M. A. Sabaawi (ahmed.sabaawi@uoninevah.edu.iq).

The authors are with the College of Electronics Engineering, Ninevah University, Mosul, Iraq.

an acceptable read range regardless the direction of incoming signals. Typical tag antennas are light weight, inexpensive, exhibit an excellent reflection coefficient and tolerant to the attached objects in order to keep the performance acceptable [3]. Normally, meandered line structures [1], spiral and inverted-F and antennas are employed [4–6]. However, fractal loop antennas have shown higher gain and stable radiation which are preferable in such applications [7–9].

In this paper, new fractal curves have been proposed as polygon shapes (5-sides, 6-sides, 7-sides, and 8-sides), and fractal loop antennas based on the 2nd iteration have been designed. The performances of these fractal loop antennas are compared with each other to find better characteristics, and compared with another fractal loop antenna proposed in literature [10, 11].

## 2. PROPOSED FRACTAL CURVE

Fractal shapes have some of their parts the same as the entire original shape but with different scales, which is so called “self-similarity” [12–15]. Some iterative algorithms such as iterated function system (IFS) may be applied infinite number of times (iterations) to build a fractal shape. This procedure can be applied to an initial structure many times but at different scales to construct the fractal shape.

Fractal antennas can adopt various fractal shapes. For example,  $\lambda/4$  monopole can become a shorter antenna by employing Koch fractal [9]. The Sierpinski gasket can also be shaped as a dipole or monopole antenna [16, 17]. In this paper, several fractal curves are proposed as fractal loop antennas in order to increase the area enclosed by the loop and hence improve the radiation characteristics of the antenna. The proposed fractal curves are 5-, 6-, 7-, and 8-sides polygon fractal shapes and have an effective length ( $l_{eff}$ ) given by:

$$l_{eff} = l \cdot (2)^n, \quad (1)$$

where ( $n$ ) is the number of iterations.

The affine transformation of the suggested 5-sides polygon fractal curve in the  $\omega$ -plane is represented in Equation (2) below, where the affine transformation is a special kind of projective transformations that preserve proportions on lines, but not distances and angles.

$$\begin{aligned} \omega &= [r \cos \theta, -r \sin \theta, r \sin \theta, r \cos \theta, e, f] \\ \omega 1 &= [1/3, 0, 0, 1/3, 0, 0] \\ \omega 2 &= [-0.103, -0.317, 0.317, -0.103, 1/3, 0] \\ \omega 3 &= [0.269, -0.195, 0.195, 0.269, 0.230, 0.317] \\ \omega 4 &= [0.269, 0.195, -0.195, 0.269, 0.499, 0.512] \\ \omega 5 &= [-0.103, -0.317, 0.317, -0.103, 0.768, 0.317] \\ \omega 6 &= [2/3, 0, 0, 2/3, 2/3, 0] \\ \omega t &= \omega 1 \cup \omega 2 \cup \omega 3 \cup \omega 4 \cup \omega 5 \cup \omega 6, \end{aligned} \quad (2)$$

where  $r$  is a scaling factor;  $\theta$  represents the rotating angle; and  $e$  and  $f$  are transformation translations.

IFS can be applied to each segment to produce additional iterations as illustrated in Fig. 1. Fig. 2 shows the first three iterations P0, P1, and P2 of the 5-sides polygon fractal curve. The same procedure can also be applied to the 6-, 7- and 8-sides polygon fractal shapes to construct more iterations of these fractal shapes.

## 3. FRACTAL LOOP ANTENNAS

Four fractal loop antennas are designed for passive UHF RFID tags operating at 900 MHz based on 5-, 6-, 7-, and 8-sides polygon fractal loops. The designed fractal loop antennas are simulated utilizing CST simulator, and their performances are compared based on resonance characteristics extracted from the return loss of each antenna as shown in Fig. 3. It is worth mentioning that the fractal loop antennas are constructed based on the 2nd iteration of the suggested fractal curves (shown in Fig. 4) with line width (1 mm) printed on a 1.6 mm thick FR-4 substrate with a dielectric constant of 4.1.

Loop antennas effectively respond to the generated magnetic flux density ( $B$ ) of the applied plane wave. The voltage induced around the loop terminals varies with the change of the magnetic flux  $\Phi$

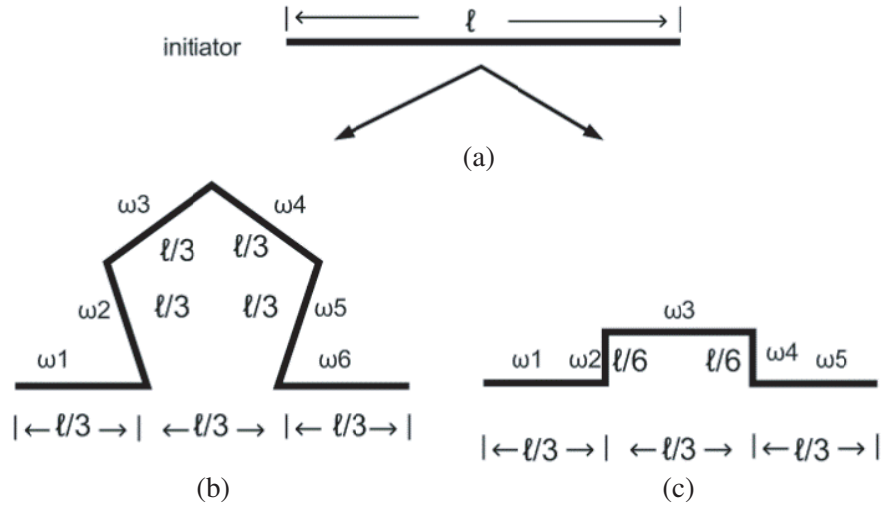


**Figure 1.** The proposed fractal curves (first iteration) compared with the fractal curve previously published in literature [10]. (a) initiator ( $n = 0$ ), (b) proposed fractal curve generator and (c) curve generator in [10].

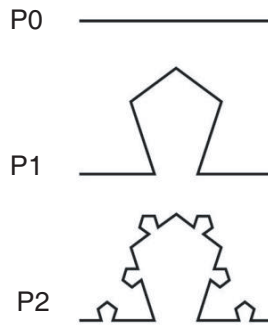


**Figure 2.** The initiator ( $P_0$ ) and the first two iterations of the proposed fractal 5-sides polygon fractal curve.

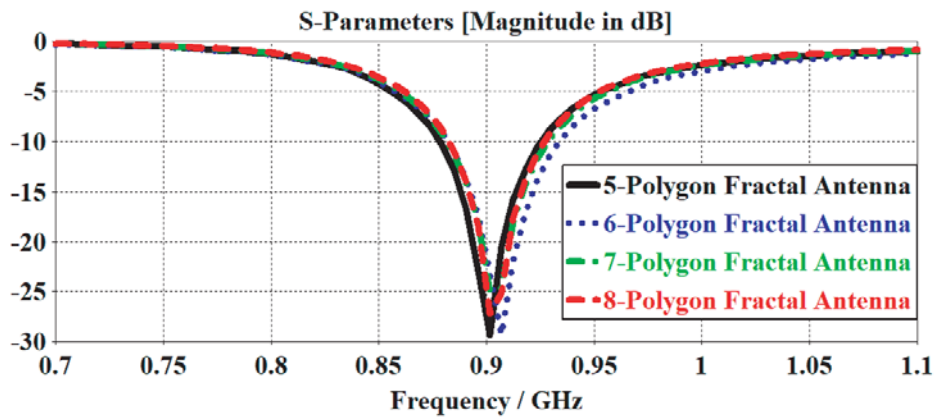


**Figure 3.** Simulated return loss ( $S_{11}$ ) for N-Polygons fractal antennas.

over time through the loop, which is basically proportional to the enclosed area ( $S$ ) by the loop, as given by [18]:

$$V \propto \frac{\partial \Phi}{\partial t} \propto \omega |\vec{B}| S \tag{3}$$

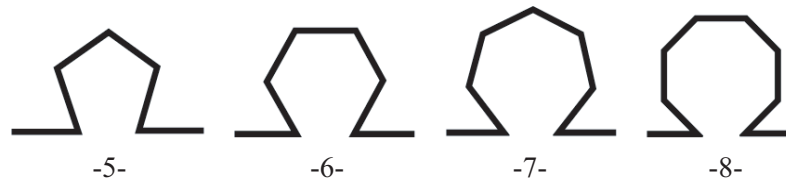


**Figure 4.** The designed fractal (5, 6, 7, 8) sides polygons.

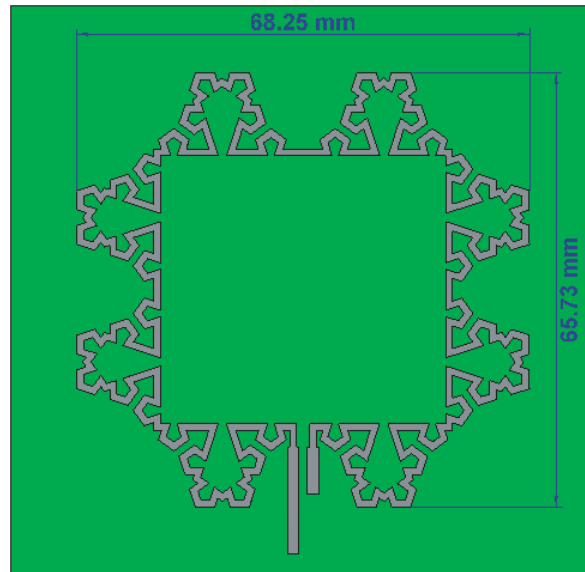


**Figure 5.** Simulated 5-Polygon fractal antenna (utilizing 2nd iteration).

Thus, increasing the enclosed area ( $S$ ) will lead to increasing the induced voltage, hence improve the read range of the tag. From Equation (3), it is clearly shown that increasing the enclosed area ( $S$ ) yields an increased voltage ( $V$ ). To this end, four fractal loop antennas are designed with different numbers of sides. The sides of the proposed polygons have been changed from 5 to 8 with the aim to increase the enclosed area by the loop and improve the antenna performance. Fig. 5 illustrates the simulated 2nd iteration of the 5-sides loop antenna showing the feeding lines and dimensions.

The 2D and 3D radiation characteristics of the 5-sides loop antenna have also been examined in this work as shown in Figs. 6 and 7. It must be clarified that the radiation characteristics of only the 5-sides loop have been reported here since the other polygons exhibit similar characteristics, and there is no need to repeat them all in order to save space throughout the manuscript. The proposed antennas exhibit an 8-shape radiation pattern similar to dipole radiation characteristics with reasonable gain and beamwidth. By increasing the enclosed area of the loop, the designed antennas showed a better performance in terms of gain than previously published works [10] and a better return loss than other works [11]. Furthermore, the designed fractal loop antennas outperformed previously published non-fractal geometries [19].

#### 4. EXPERIMENTAL RESULTS

The designed fractal loop antennas have been fabricated using PCB technology on an FR-4 substrate layer as shown in Fig. 8. A quarter wavelength bazooka balun has been implemented at the input terminal of the fabricated loop antennas by adding a short-circuited sleeve at the outer conductor of the feeding coaxial cable for the purpose of achieving balanced currents. The return loss of the fabricated antennas was measured using network analyzer over a range of frequencies 0.7–1 GHz as depicted in

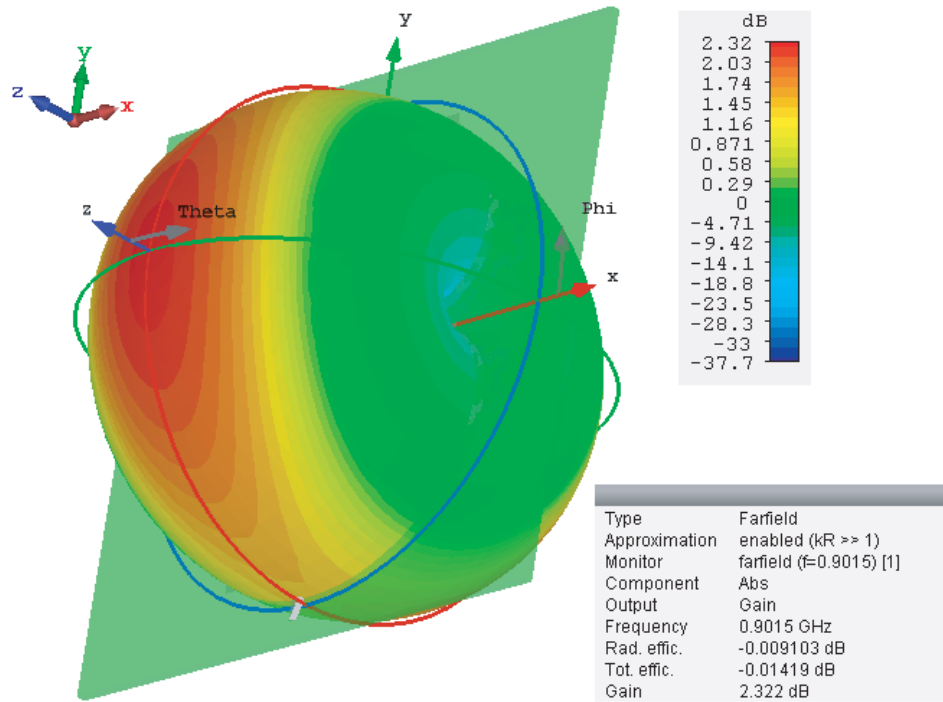


Figure 6. Simulated 3-D plot of radiation pattern for 5-Polygon fractal loop antenna.

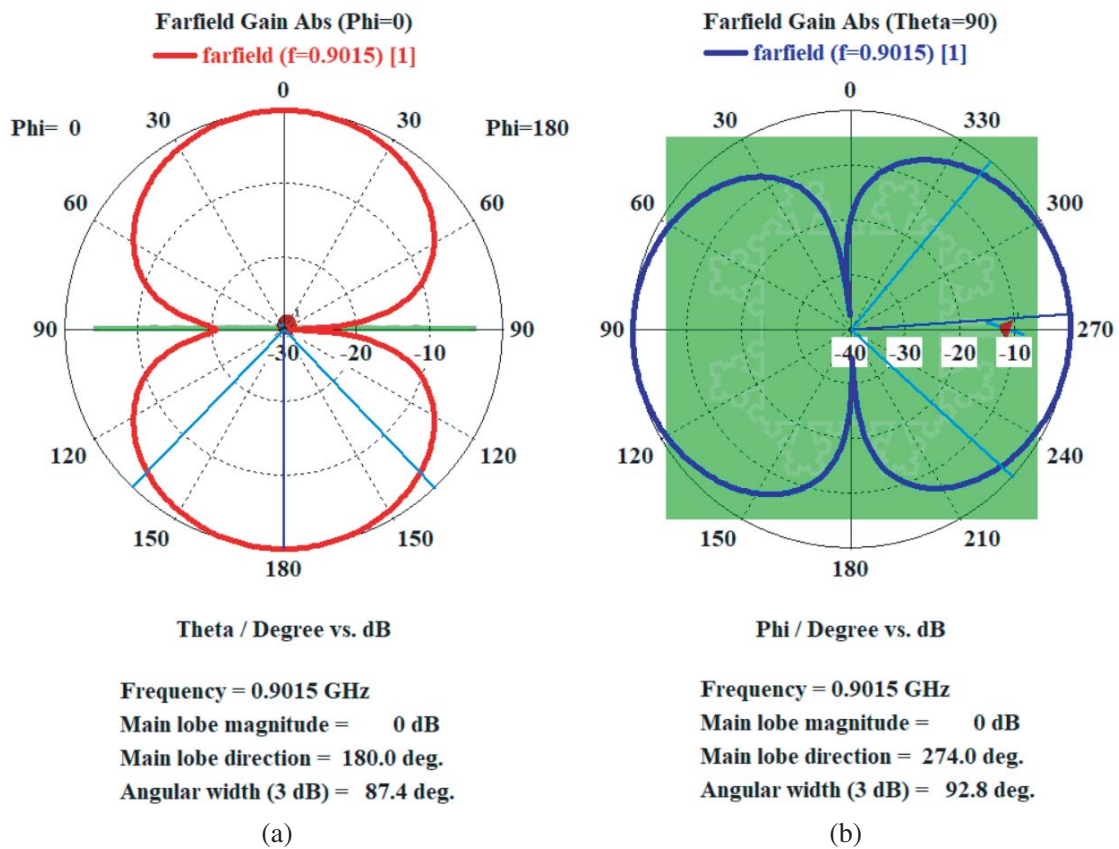
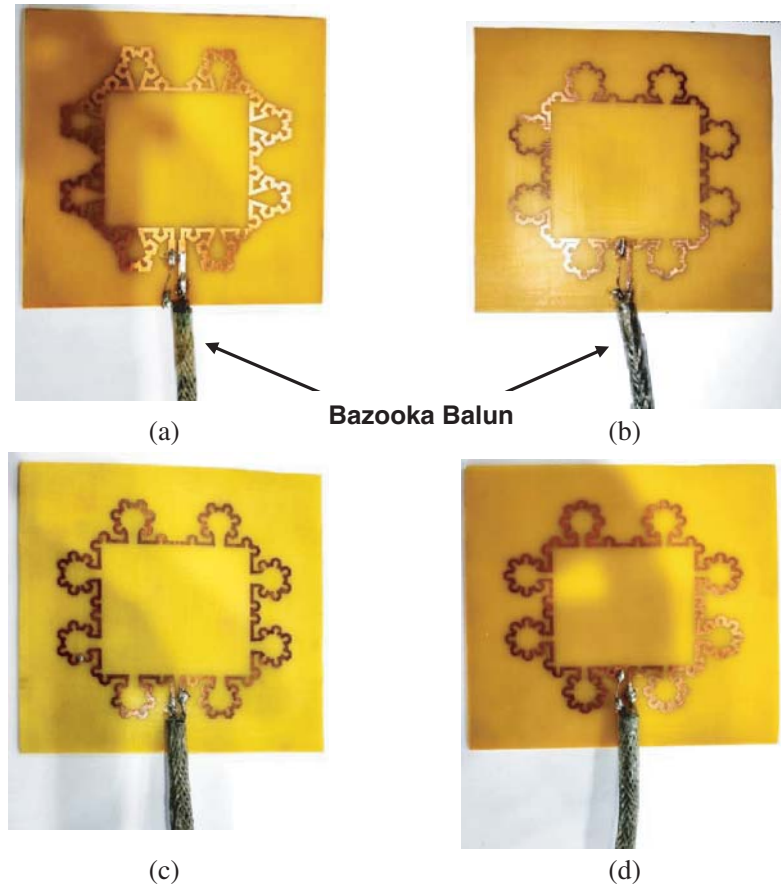
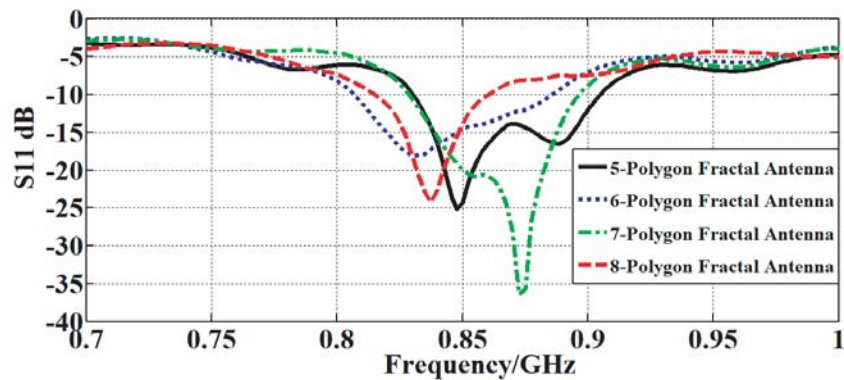


Figure 7. Simulated polar plot of radiation pattern at *E* and *H* plane for 5-Polygon fractal loop antenna. (a) *E*-plane. (b) *H*-plane.



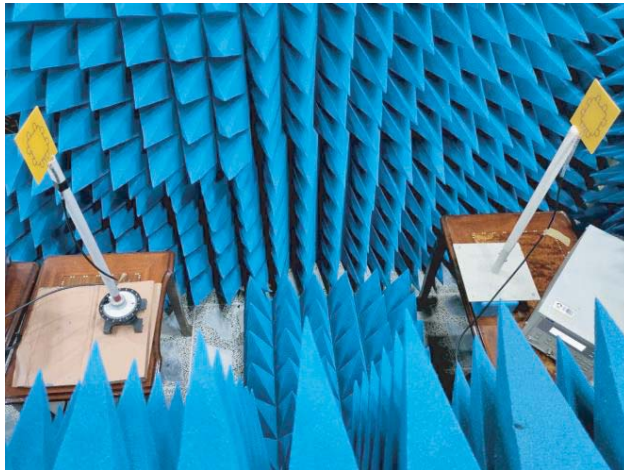
**Figure 8.** Fabricated fractal loop antennas: (a) 5-sides polygon, (b) 6-sides polygon, (c) 7-sides polygon and (d) 8-sides polygon.



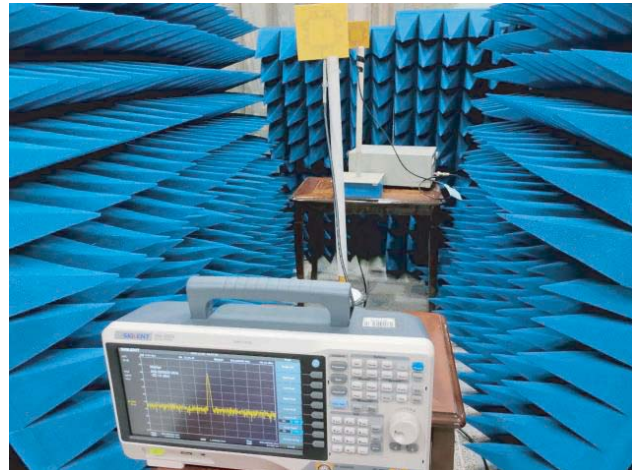
**Figure 9.** Measured return loss for N-Polygons fractal antennas measured by VNA,  $N = 5, 6, 7, 8$ .

Fig. 9.

It can be seen from Fig. 9 that the fabricated antennas resonate at frequencies below 900 MHz, and the resonant frequencies for the fabricated antennas are different from each other. The reason behind these differences might be the difference in dielectric constant value between simulation and measurements. Another reason could be the perturbation of impedance at the input terminals (feeding point) of the loop antenna. However, the fabricated antennas still resonate at 900 MHz and can work properly with passive UHF RFID tags. It is worth mentioning that two identical copies of each antenna



**Figure 10.** Experimental setup showing the transmitting antennas with the installed absorbers.



**Figure 11.** Experimental setup for measuring the gain and radiation pattern.

were fabricated for the purpose of measuring the gain.

The radiation pattern and gain of the fabricated antennas have also been measured using microwave source and spectrum analyzer along with two identical copies of each antenna. Anechoic absorbing material has been used to eliminate reflections during the measurement process as shown in the experimental setup in Figs. 10 and 11. Table 1 compares the measured and simulated gains of the suggested fractal loop antennas. Fig. 12 shows the measured 2D radiation patterns for all fabricated antennas compared with their simulated results. It is clearly observed that there is excellent agreement between simulated and measured radiation patterns. Although 6-Polygon antenna has higher BW in air than other iterations; however, the figure of merits in this application depends on the materials to be tagged where other antennas showed better performance as will be explained later in Section 5.

**Table 1.** Simulated and measured gain of the proposed fractal loop antennas.

	5-Polygon	6-Polygon	7-Polygon	8-Polygon
<b>Simulated Gain dB</b>	2.32	2.38	2.29	2.26
<b>Measured Gain (dB)</b>	1.85	1.50	1.56	1.55

In order to examine the gain performance of the designed antennas over a wide range of frequencies, the gain versus frequency was plotted over a frequency range from 800 MHz to 1000 MHz as shown in Fig. 13. The simulation result shows that the four designed fractal antennas exhibit a stable performance in terms of gain, and the observed change for the 200 MHz (0.8 GHz–1 GHz) was trivial. It has also seen that 6-Polygon fractal loop antenna has recorded higher simulated gain at all frequencies of interest than other antennas.

## 5. EFFECT OF DIFFERENT MATERIALS ON ANTENNA PERFORMANCE

RFID tags are normally placed on the objects to be identified. The materials of these objects may alter the performance of the RFID tag antenna due to the change in the resonance frequency and bandwidth [18, 20]. Thus, the performance alteration due to placing the tag on different objects must be studied extensively in order to obtain comprehensive understanding of such performance changes. To this end, the fabricated antennas were placed on different materials, and their return losses were measured and depicted in Fig. 14. Table 2 presents a full comprehensive analysis of the effect of different

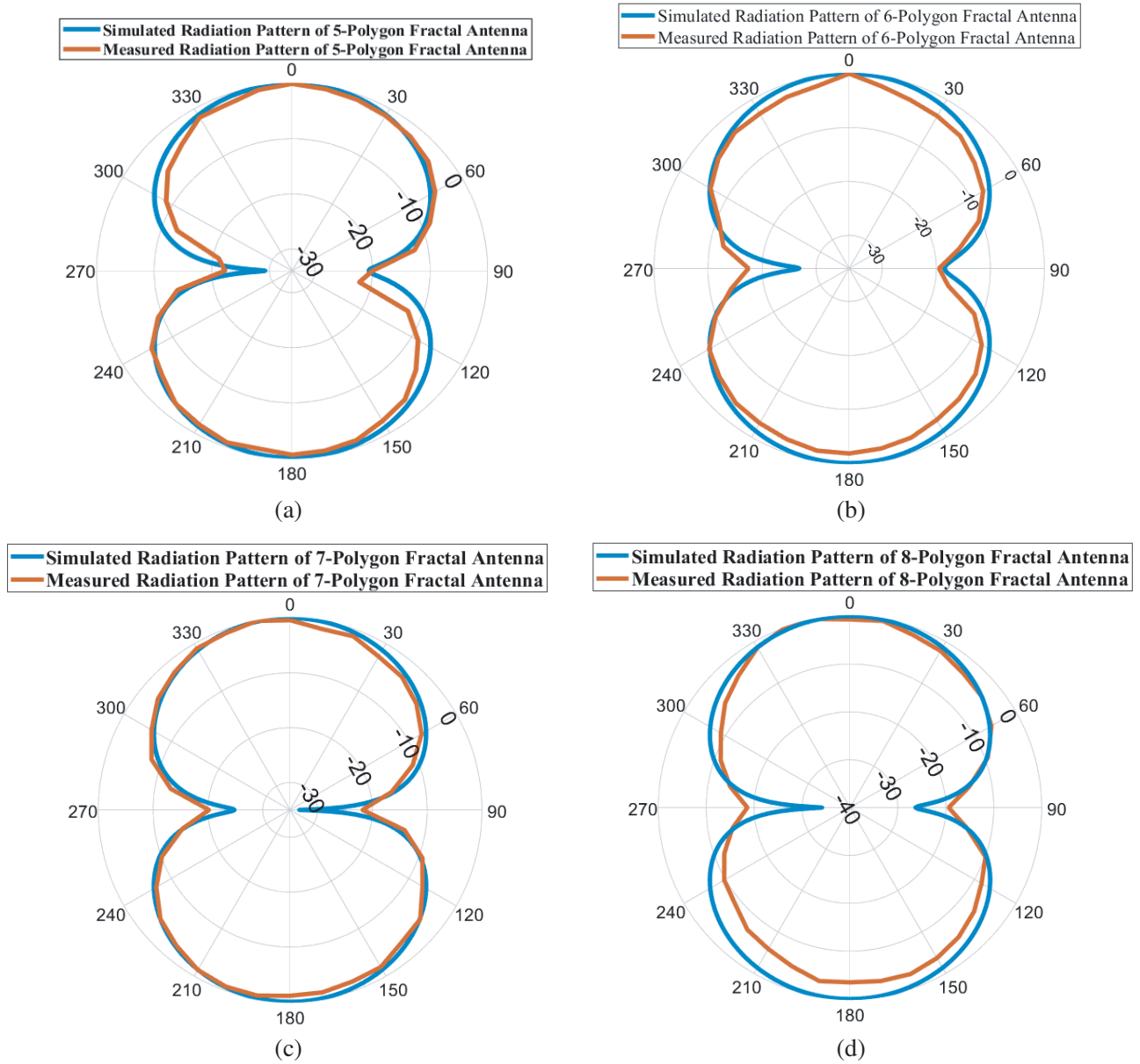


**Figure 12.** Simulated and measured radiation pattern (normalized) of the designed and fabricated fractal loop antennas: (a) 5-Polygons, (b) 6-Polygons, (c) 7-Polygons and (d) 8-Polygons.

materials on the antenna performance as well as shows the difference in resonant frequency ( $f_r$ ) and bandwidth (BW) when antennas are placed on different objects. The value of  $\Delta f$  is given by subtracting the resonant frequency for the antenna when it is placed on an object from the value of the resonant frequency of the antenna in air ( $\Delta f = f_r(\text{on material}) - f_r(\text{in air})$ ).

A closer look at Table 2 reveals that the resonant frequency of the antennas is shifted when the antenna is placed on an object; however, it is noticed that cork has the minimum impact while water has notably significant impact on the resonant frequency. On the other hand, the frequency bandwidth is also influenced by placing the antenna on an object, but in some cases the bandwidth is rather improved, which is preferable in this application. Furthermore, it is clearly noticed that the 8-Polygon Fractal Antenna outperformed other types (in terms of  $\Delta f$ ) when being placed on cardboard and metal, whereas the 6-Polygon Fractal Antenna outperformed other types when being placed on cork and wood. In addition, the 5-Polygon Fractal Antenna performed well on nylon while the 7-Polygon Fractal

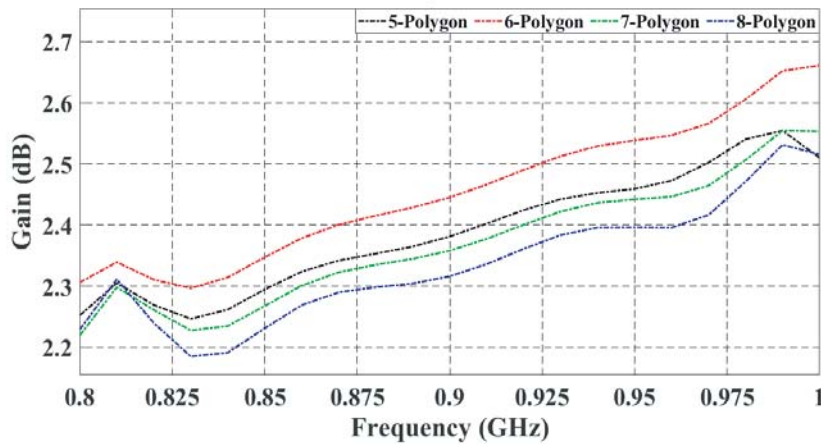


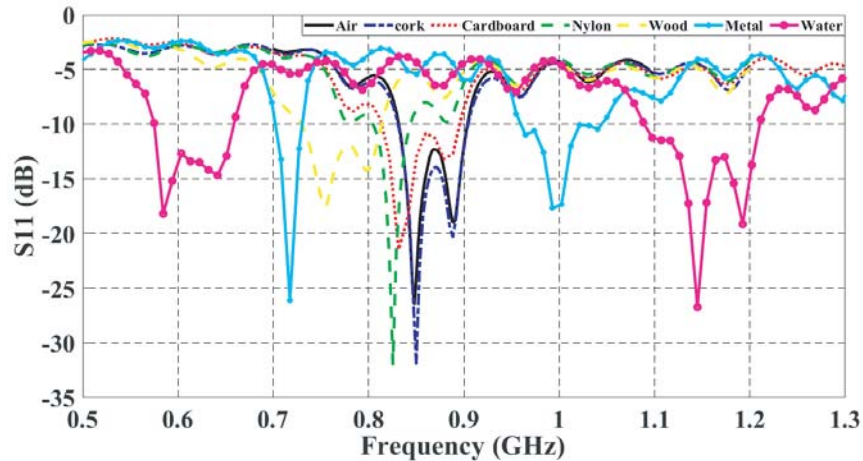
Figure 13. Simulated results of gain vs frequency for N-Polygons fractal antennas by CST  $N = 5, 6, 7, 8$ .

Table 2. Effect of different material on the antenna performance.

Antenna Type	Air	cork	Cardboard	Nylon	Wood	Metal	Water	
5-Polygon Fractal Antenna	$f_r$ (MHz) =	848	850	831	825	755	717	584
	$B.W$ (MHz) =	72	74	82	39	85	28	83
	$S_{11}$ (dB) =	-27	-31.9	-21.5	-31.7	-17.6	-26	-18.2
	$\Delta f$	0	2	-17	-23	-93	-131	-264
6-Polygon Fractal Antenna	$f_r$ (MHz) =	850	850	831	822	780	N/A	537
	$B.W$ (MHz) =	67	67	47	39	73	N/A	44
	$S_{11}$ (dB) =	-21	-21.3	-15.7	-33.4	-13.6	N/A	-21.5
	$\Delta f$	0	0	-19	-28	-70	N/A	-313
7-Polygon Fractal Antenna	$f_r$ (MHz) =	880	871	850	832	762	736	668
	$B.W$ (MHz) =	66	64	66	62	56	23	44
	$S_{11}$ (dB) =	-25	-33	-19.7	-13.8	-18.9	-16.6	-64.9
	$\Delta f$	0	-9	-30	-48	-118	-144	-212
8-Polygon Fractal Antenna	$f_r$ (MHz) =	965	958	955	864	860	898	N/A
	$B.W$ (MHz) =	69	73	64	122	64	22	N/A
	$S_{11}$ (dB) =	-21	-17.5	-16.3	-13.2	-18.3	-11.8	N/A
	$\Delta f$	0	-7	-10	-101	-105	-67	N/A

N/A: means that the measured resonant frequency is out of range for the UHF RFID technology, so it has been excluded from the results.

Antenna showed a better performance on water than other types. Hence, this comprehensive study helps identifying the best candidate RFID antenna based on the objects to be tagged. Additionally, by knowing the influence of different materials, the designer could have a clear image on the possible shift in resonant frequency and hence design the antenna with a fine tuning capability to overcome this issue. It is worth mentioning that the fabricated antennas were attached directly (i.e., no spacing distance) to the materials to be tagged, and the area of materials under the antenna was almost 2–3 times of the antenna’s area to ensure a practical case study similar to reality.



**Figure 14.** Measured return loss for the proposed 5-Polygon fractal antenna when it is mounted on various materials.

## 6. CONCLUSION

In this work, four fractal curves are proposed and have been used as a fractal loop antennas for 900 MHz passive UHF RFID tags. The designed fractal loop antennas were validated numerically by utilizing CST electromagnetic simulator. The return loss, gain, and 2D and 3D radiation patterns of the simulated loop antennas were presented and discussed. The proposed fractal loops were also fabricated on PCB substrates, and their characteristics were measured experimentally in a semi-anechoic environment. The measured results agreed well with the simulated values. The proposed fractal loop antennas have better radiation properties than those published previously and have higher read range because they enclose larger area, and they have a smaller size. It is also shown that increasing the number of polygon sides could cause decrease in the size of the antenna and keeps the most quality of radiation pattern at the same resonant frequency. The influence of various materials on the antenna performance was extensively investigated. It was shown that the antenna kept an acceptable performance even if it has been attached to different object materials.

## REFERENCES

1. Salama, A. M. A. and K. Quboa, "Fractal dipoles as meander lines antennas for passive UHF RFID tags," *Proceedings of the Fifth International Multi-Conference on Systems, Signals and Devices (IEEE SSD'08)*, Vol. 3, 128, Jordan, July 2008.
2. Babaeian, F. and N. C. Karmakar, "Time and frequency domains analysis of chipless RFID back-scattered tag reflection," *IoT 1*, No. 1, 109–127, 2020.
3. Rokunuzzaman, Md., M. T. Islam, W. S. T. Rowe, S. Kibria, M. J. Singh, and N. Misran, "Design of a miniaturized meandered line antenna for UHF RFID tags," *PloS One 11*, No. 8, e0161293, 2016.
4. Ukkonen, L., L. Sydanheimo, and M. Kivikoski, "A novel tag design using inverted-F antenna for radio frequency identification of metallic objects," *Proc. 2004 IEEE/Sarnoff Symp. Advances in Wired and Wireless Communication*, 91–94, April 2004.
5. Riaz, M., G. Rymar, M. Ghavami, and S. Dudley, "A novel design of UHF RFID passive tag antenna targeting smart cards limited area," *2018 IEEE International Conference on Consumer Electronics (ICCE)*, 1–4, IEEE, 2018.
6. Werner, D. H. and S. Ganguly, "An overview of fractal antenna engineering research," *IEEE Antennas and Propagation Magazine*, Vol. 45, No. 1, 38–56, February 2003.

7. Zeng, M., A. S. Andrenko, X. Liu, H.-Z. Tan, and B. Zhu, "Design of fractal loop antenna with integrated ground plane for RF energy harvesting," *2016 IEEE International Conference on Mathematical Methods in Electromagnetic Theory (MMET)*, 384–387, IEEE, 2016.
8. Sabaawi, A. M. A. and K. M. Quboa, "Design and fabrication of miniaturized fractal antennas for passive UHF RFID tags," *Advanced Radio Frequency Identification Design and Applications*, 2010.
9. Sabaawi, A. M. A. and K. M. Quboa, "Wideband modified dipole antenna for passive UHF RFID tags," *2010 7th International Multi-Conference on Systems, Signals and Devices*, 1–4, IEEE, 2010.
10. Salama, A. M. A. and K. Quboa, "A new fractal loop antenna for passive UHF RFID tags applications," *Proceedings of the 3rd International Conference on Information & Communication Technologies: From Theory to Applications (ICTTA'08)*, 477, April 7–11, 2008.
11. Sultan, Q. H. and A. M. A. Sabaawi, "Design a new fractal loop antenna for UHF RFID tags based on a proposed fractal curve," *2010 2nd International Conference on Computer Technology and Development*, 6–9, IEEE, 2010.
12. Orazi, H. and H. Soleimani, "Miniaturisation of the triangular patch antenna by the novel dual-reverse-arrow fractal," *IET Microwaves, Antennas & Propagation*, Vol. 9, No. 7, 627–633, 2014.
13. Anguera, J., C. Puente, C. Borja, and J. Soler, "Fractal-shaped antennas: A review," *Wiley Encyclopedia of RF and Microwave Engineering*, Vol. 2, edited by K. Chang, 1620–1635, 2005.
14. Werner, D. H. and S. Ganguly, "An overview of fractal antenna engineering research," *IEEE Antennas and Propagation Magazine*, Vol. 45, No. 1, 38–57, February 2003.
15. Anguera, J., A. Andújar, J. Jayasinghe, V. V. S. S. S. Chakravarthy, P. S. R. Chowdary, T. Ali, J. L. Pijoan, and C. Cattani, *Fractal Antennas: An Historic Perspective*, Fractal and Fractional, 2020.
16. Yu, Z., J. Yu, X. Ran, and C. Zhu, "A novel Koch and Sierpinski combined fractal antenna for 2G/3G/4G/5G/WLAN/navigation applications," *Microwave and Optical Technology Letters*, Vol. 59, No. 9, 2147–2155, 2017.
17. Andrenko, A. S., "Conformal fractal loop antennas for RFID tag applications," *IEEE Applied Electromagnetics and Communications, ICECom. International Conference*, 1–6, October 2005.
18. Choi, W., H. W. Son, J. Choi, C. S. Pyo, and J. S. Chae, "An RFID tag using a planar inverted-F antenna capable of being stuck to metallic objects," *ETRI Journal*, Vol. 28, No. 2, 216–218, April 2006.
19. Salama, A. M. A., "Antennas of RFID tags," *Radio Frequency Identification Fundamentals and Applications Design Methods and Solutions*, 93–110, 2010.
20. Dobkin, D. M. and S. M. Weigand, "Environmental effects on RFID tag antennas," *IEEE Microwave Symposium Digest*, 4, June 2005.